University of Baghdad
College of Engineering
JE
JOURNAL OF ENGINEERING

Journal of Engineering
journal homepage: www.jcoeng.edu.iq
Volume 32 Number 2 February 2026

Single-Mode Optical Fiber Coated with Carbon-quantum Dots for Chemical Sensing Applications

Ola Mahdi Alwan *, Soudad S. Ahmed

Department of Physics, College of Science, University of Baghdad, Baghdad, Iraq

ABSTRACT

This study presents the design and fabrication of a single-mode optical fiber-based sensor capable of identifying different concentration levels of acetic acid solutions. Carbon quantum dots were deposited onto the core region of the optical fiber following chemical etching of the cladding layer using hydrofluoric acid (HF). The sensor was evaluated using five acetic acid concentrations (10, 15, 18, 20, and 25%) to determine its sensitivity based on variations in resonance wavelength and optical transmission. When exposed to larger concentrations, the sensor clearly showed a red shift in resonance wavelength, indicating a direct correlation between the optical response of the sensor and the refractive index of the detecting medium. Since traditional methods frequently have low sensitivity and large instrumentation. There is an increasing demand for a small and extremely sensitive approach to detect acetic acid. Spectral and intensity analyses confirmed the sensor's performance, showing a sensitivity measurement of 10 μm/RIU and an established ratio of signal-to-noise of 0.14. Surface Plasmon Resonance (SPR) is the main basis for the sensing mechanism enabled by the relationship between the fiber's evanescent field and the carbon quantum dot coating. The testing results establish that the sensor performs efficiently in detecting liquid chemicals, especially acetic acid and related organic substances. A specially fabricated tapering setup was employed to enhance the sensor's responsiveness to changes in the surrounding refractive index. A short-tapered segment of single-mode fiber, approximately 4 cm in length, was formed at the center of the sensor. The tapered region, with carefully controlled cladding diameter and length, was exposed to acetic acid solutions with different concentrations in order to monitor variations in the effective refractive index (RI).

Keywords: Single-mode fiber, Surface-plasmon-resonance, Acetic acid sensing.

1. INTRODUCTION

Many applications in communication, scientific projects, and environmental monitoring use optical fiber sensors since they are small, responsive, electrically balanced, immune to electromagnetic interference, and can handle wide bands of frequencies **(Mahmood and Ahmed, 2018; Yasser et al., 2018)**. Initially, researchers proposed using optical fibers for surface plasmon resonance (SPR) sensing in **(Jorgenson and Yee, 1993)**. SPR has seen

*Corresponding author
Peer review under the responsibility of University of Baghdad.
https://doi.org/10.31026/j.eng.2026.02.09

Article received: 04/09/2025
Article revised: 05/01/2026
Article accepted: 20/01/2026
Article published: 01/02/2026

important advancements in sensor performance after starting to use optical fiber technology. Today, Fiber-optic sensors that rely on surface plasmon resonance (SPR) are popular for applications since they are fast-responding, less sample-absorbing, don't need labels, fit nicely in small devices, and are remotely observable in real time **(Jorgenson and Yee, 1993; Homola, 1995).** In optical fiber systems, information is transmitted through light pulses propagating along the fiber. Electrical signals are first converted into optical signals at the transmitter end. The propagation mechanism relies on total internal reflection at the core–cladding interface, allowing light to remain confined within the core and travel over long distances with minimal attenuation **(Jassam, 2024)**

The basic principle of SPR is that light entering a metallic layer stirs interactions with its free electrons. When the electrons in a metal vibrate at the same rate as the incoming light, reflected light is diminished. The photon enters the metal and causes a surface plasmon wave to be produced. **(Nesterenko and Sekkat, 2013; Hottin et al., 2013)**. Surface plasmon action can be acquired with a variety of devices including low-index prisms, diffraction gratings, and optical fibers **(Srivastava and Gupta, 2011).**

Surface plasmon resonance (SPR) paired with optical fiber systems has made it achievable to develop sensors that are far more sensitive for chemical and biological detection. Owing to their ability to provide real-time measurements, compact structure, and adaptability, these sensors have attracted considerable attention in applications such as medical diagnostics and environmental analysis. With ongoing technological progress, SPR-based optical fiber sensors are anticipated to achieve improved performance and broader practical implementation **(Abdul Kareem and Ahmed, 2023).**

By altering the surface of different fiber shapes coting depositing methods increase the sensing qualities of optical fiber sensors. **(Urrutia et al., 2015)**. When coating fibers with carbon-based nanomaterials including graphene, carbon nanotubes (CNTs), and carbon quantum dots (CQDs), which have superior electrical, optical, and chemical properties, optical fiber surface modification is a successful technique for increasing sensor efficiency. **(Gupta, 2006; He et al., 2008).** Quantum dots (QDs) are spherical Semiconductor nanocrystals with size dependent florescence that range in size from 1 to 2 nm. However, metal-based QDs are poisonous and expensive. Originally discovered during the purification of carbon nanotubes, carbon dots provide a low-toxicity, environmentally friendly utilized in sensing and energy-related applications **(Ateia et al., 2024)**. Carbon coatings strengthen the interaction between the surrounding analyte and the evanescent field, improving sensor sensitivity and selectivity **(Nacpil et al., 2019).** Furthermore, these nanomaterials are appropriate for chemical and biological sensing applications because they have functional groups that enable selective interaction with target molecules **(Ding et al., 2017).** Recent research indicates that carbon-coated tapered optical fibers are excellent high-performance chemical sensors for real-time monitoring of biomolecules and environmental contaminants. **(Yao et al., 2020; Wu et al., 2016).** Although SPR traditionally relies on noble metals such as gold and silver due to their free-electron oscillations at the metal–dielectric interface, recent advancements in nanomaterials have shown promising alternatives. Carbon quantum dots (CQDs) and graphene are examples of materials that can behave like plasmons, particularly in the infrared spectrum **(Low and Avouris, 2014).** Numerous biosensing techniques, such as optical, electrochemical, thermometric, piezoelectric, and magnetic methods, have been investigated. Among these, surface plasmon resonance (SPR) spectroscopy has become widely used because of its sensitivity and adaptability in chemical and biological studies. SPR-based sensors have gained widespread recognition in scientific

study since their initial use in biosensing and gas detection in 1982. Light interaction at surfaces between materials with different refractive indices is the fundamental idea behind SPR. When the angle of incidence surpasses a crucial value, light going from a media with a higher refractive index, like glass, to one with a lower one, like air, experiences total internal reflection. Reflected light can couple with surface plasmons on the metal surface by depositing a tiny coating of metal, usually gold, at the contact **(Daniyal et al., 2025).** These nanomaterials use their unique optical and electrical properties, such as tunable permittivity, strong light confinement, and quantum confinement effects, to produce similar resonance phenomena instead of relying on classical electron oscillations in metals. This allows for the creation of sophisticated, effective, and tunable optical sensors **(Yan et al., 2013; Kumawat et al., 2019; Wang and Hu, 2019).**

This work aims to create a taper-based single-mode optical fiber sensor by applying a carbon quantum dot coating. The sensor makes use of the increased surface area caused by tapering and the unique sensing properties of CQDs to detect changes in the refractive index and concentrations of acetic acid solutions.

2. CARBON QUANTUM DOTS

Due to quantum confinement effects and their small particle size, usually between 2 and 10 nm, emerging carbon-based nanomaterials known as carbon quantum dots (CQDs) have unique optical and electrical properties. Their powerful photoluminescence is well-known **(Yola and Atar, 2020)**, They are suitable for a number of applications due to their exceptional chemical stability, low toxicity, and water solubility. in the domains of optical sensing, bioimaging, and energy **(Xu et al., 2014).** The remarkable optical of CQDs stem from their quantum confinement and the presence of functional groups on their surface, such as hydroxyl and carboxyl, which allow them to generate intense fluorescence across a wide spectrum and absorb light. By adjusting the surface, size, chemistry, or synthesis circumstances, this emission can be adjusted **(Li et al., 2020).** CQDs react rapidly visually when their chemical environment changes, such as when pH shifts or metal ions are present **(Zhu et al., 2015).** These characteristics make them highly desirable for optical sensor design. A helpful nanocoating material for fiber optic sensing is CQDs. When applied to tapered optical fibers, they enhance the enhancement of light absorption and spectrum responsiveness through the interaction of the evanescent field with the external medium. This leads to improved sensitivity and detection accuracy in chemical and biological sensing applications **(Baker and Baker, 2010).**

3. PERFORMANCE PROPERTIES

Sensitivity, figure of merit, signal-to-noise ratio, and resolution were among the performance factors that were examined. Spectral interrogation was used to measure sensitivity (S), which is the resonance wavelength shift that occurs with each change in the refractive index of the sensing medium, as shown by equation **(Wang et al., 2021):**

$$\boldsymbol{S = \frac{\Delta\lambda_{res}}{\Delta n_s}} \quad (1)$$

$\Delta\lambda_{res}$ and Δn_s represent the changes in resonance wavelength and refractive index, respectively. This means, according to this formula, that the sensitivity is in (nm/RIU). According to reference **(Abbas and Ahmed, 2023),** the amount of depth that the spectral

curve observes transforms into a lesser SNR (Signal-to-noise ratio) and FOM (Figure of merit).

$$SNR\ (n)\ =\ [\frac{\Delta\lambda_{\text{res}}}{\Delta\lambda_{0.5}}] \tag{2}$$

Where $\Delta\lambda_{0.5}$ is the spectral curve breadth.

$$FOM = \frac{\text{s}}{\Delta\lambda_{0.5}} \tag{3}$$

The sensor's lowest detectable is the resolution of the refractive index change, referred to as the sensor, and it is as follows **(Jassam et al., 2024):**

$$R\ =\ \frac{\Delta n_{\text{s}}}{\Delta\lambda_{\text{res}}}\Delta\lambda_{\text{DR}} \tag{4}$$

Where $\Delta\lambda_{DR}$ is the spectral resolution. Although these equations are usually used for metals (surface plasmon resonance), the same method was utilized to assess the carbon-based sensor's performance. A change in the resonance wavelength was observed with changes in the sample, and this shift was used to assess the response of the carbon-based sensor. Although carbon quantum dots (CQDs) are not metals in the conventional sense, they can exhibit localized surface plasmon-like resonance due to their unique optical and electronic characteristics. Therefore, they were considered in the design of the plasmonic sensor in a similar role to metallic layers.

4. MATERIALS AND METHOD

In the following section, we will focus on the material and methods that are used in this work.

4.1 Carbon Quantum Dots Preparation

Electrochemical methods enabled the synthesis of Carbon Quantum Dots (CQDs). All necessary chemicals were obtained from Merck, including C_2H_5OH and NaOH, for the experiment. The NaOH solution achieved full dissolution by maintaining constant agitation with a magnetic stirrer throughout 15 minutes period. The solution was moved to the following graphite rod position**.** A 250 mL beaker with an attached power supply received the solution afterwards. The solution contained graphite rods that measured one inch and stayed separated by approximately 2 cm from each other. Ion movement between the electrodes was facilitated through polarity switching every 5 minutes, as demonstrated in **Fig. 1**.

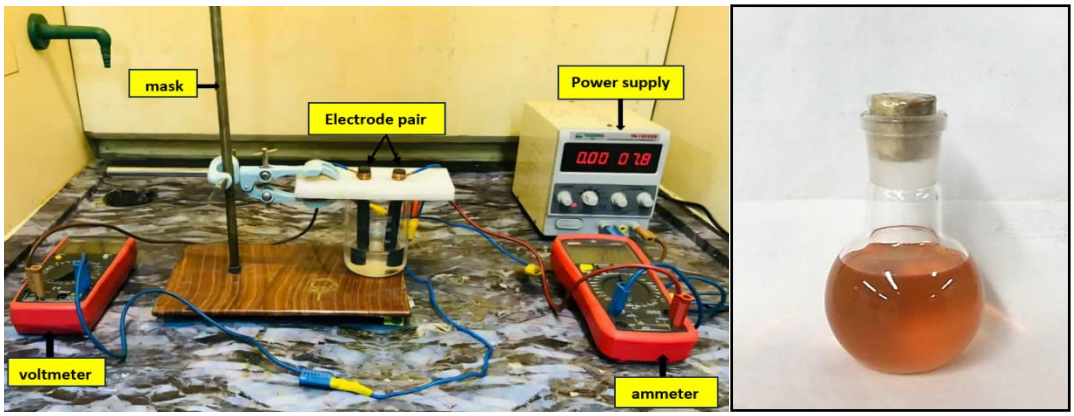

Figure 1. The setup used in this study and the solution

The completed process allowed for the collection of the solution into labeled vials before sealing them. The solution remained untouched for 5 days until it developed a yellow-orange color **(Abd and Ibrahim, 2022).**

4.2 X-Ray Diffraction Results of CQD Film

Using an X-ray diffraction pattern, the crystalographic orientation of CQDs was examined at a scanning range (2θ) from 0 to 600. The prepared CQDs' polycrystalline structure is demonstrated by these figures. Numerous diffraction peaks and a prominent orientation peak at 2θ = 32 °, which is part of the cubic structure's (111) diffraction line in **Fig. 2,** mA current, were visible in the X-ray diffraction patterns. Moreover, the patterns contained no imperfections. Additionally, the diffraction peak was intense and extremely crisp, allowing this synthesis technique to produce high-purity cubic CQDs **(Abd and Ibrahim, 2022; Thakur and Kumar, 2024).**

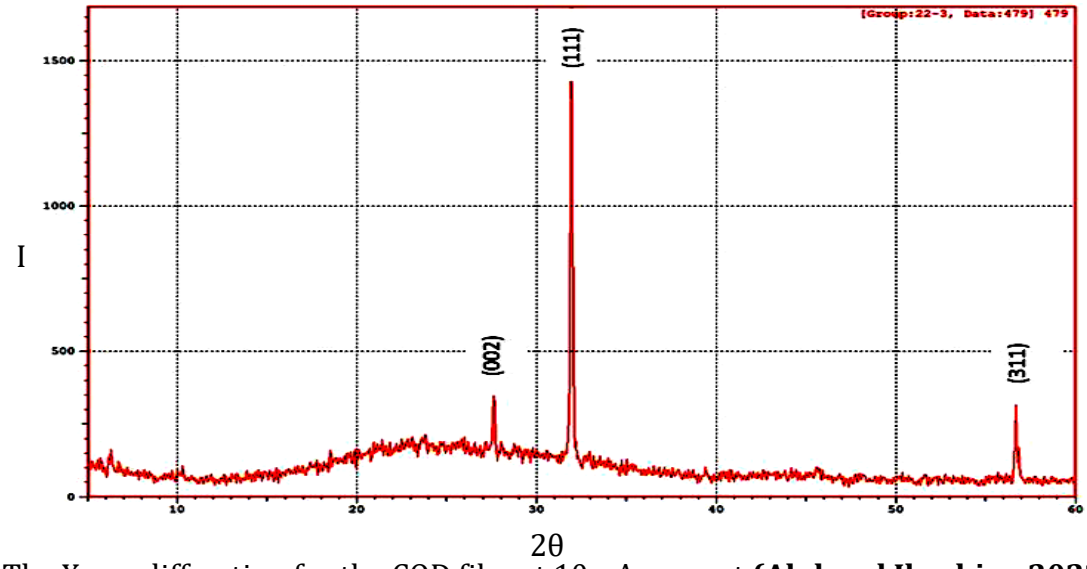

Figure 2. The X-ray diffraction for the CQD film at 10mA current **(Abd and Ibrahim, 2022; Thakur and Kumar, 2024).**

4.3 Scanning Electron Microscopes

The inset image displays agglomeration of CQDs in the 20 nm range, although the produced particles are roughly spherical. The shape of the produced particles is roughly spherical, with a grain size of 22 nm, according to SEM scans of CQDs. Many crystals are present in this grain size value, which represents the difference between the grain size and crystal size (CQD size) The cracking patterns observed in the SEM background are attributed to the drying and shrinkage of the carbon quantum dot (CQD) film on the substrate during sample preparation. Surface tension causes stress in the thin deposited layer during solvent evaporation, which leads to microcracks. These cracks are unrelated to flaws in the CQD particles and are frequently seen in dried nanomaterial films. The prepared CQDS' surface morphology, as determined by SEM at 500 nm magnification, is displayed in **Fig. 3 (Jiang et al., 2021; Tuerhong et al., 2022).**

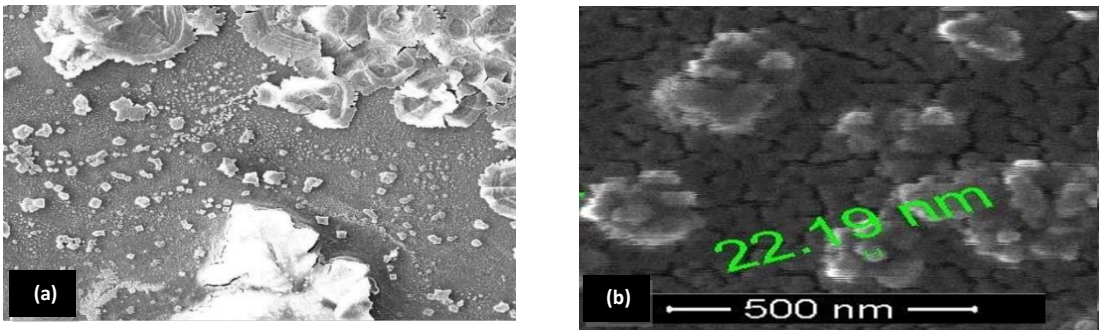

Figure 3. Particle-size distribution diagrams and SEM images of carbon quantum dots prepared at various hydrothermal reaction times.

4.4 Optical Sensor Systems

In this experiment, a 40 cm long single-mode optical fiber with a 125 μm cladding diameters and a 9 μm core was used. The protective jacket was removed from a 4 cm length of fiber in its middle section. The fiber section measuring 10 mm received a 40-minute chemical etching treatment with hydrofluoric acid (HF) to decrease its diameter. The controlled chemical etching of the fiber's core or cladding produces a narrower cross-sectional area in a tapered section. The exposed section received polishing treatment followed by cleaning with distilled water. The tapered fiber needed for SMF diameter measurement was placed on a glass plate for examination using an optical microscope. **Fig. 4** demonstrates how the acid treatment decreased the fiber diameter from 125 to 75.6 μm.

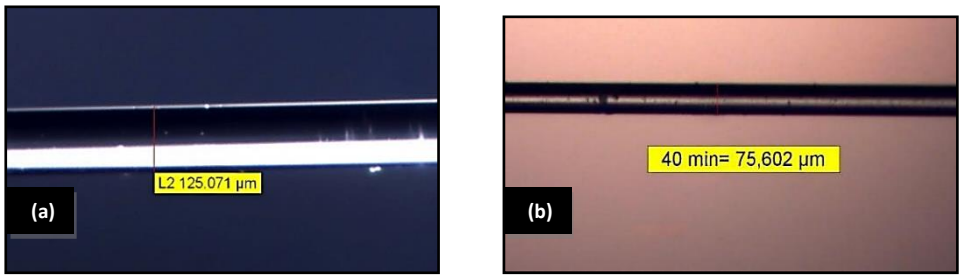

Figure 4. The images of single-mode optical fiber with a 40x magnification both before and after it has been cut to a diameter of 75.6 μm.

4.5 Deposition and Thickness Measurement of Carbon Quantum Dot Layer

The drop-casting process was carefully controlled to ensure uniform coating thickness along the tapered region. A fixed volume of the CQD solution (typically 3–5 μL) was dispensed onto the fiber using a calibrated micropipette, and the fiber was positioned horizontally to prevent solution flow or accumulation at the edges. By letting the sample dry at room temperature in a steady environment free from airflow disturbances, the evaporation rate was maintained, as shown in **Fig. 5**, these steps helped reduce thickness fluctuation and guarantee repeatability of the deposited 13.1 μm carbon quantum dot layer that was applied to the tapered segment of the optical fiber and allowed to dry.

The thickness of the deposited layer was measured using optical microscopy (Olympus BX53), by comparing the fiber diameter before and after deposition. The resulting thickness was calculated based on this measurement, as illustrated in **Fig. 6.**

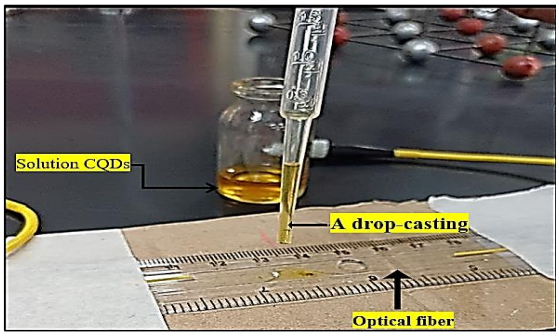

Figure 5. A drop-casting method

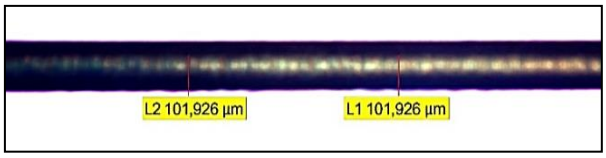

Figure 6. The images of the optical fiber after adding carbon, with magnification of 40x.

4.6 Work and Experimental Setup

The setup for transmitted light spectrum evaluation includes a 650 nm diode laser with a single-mode glass optical fiber and Thorlabs' optical spectrum analyzer. The spectrophotometer used was a CCS series from Thorlabs (Germany). It operates over a wavelength range of 200–1000 nm with a signal-to-noise ratio of ≤2000:1. The compact device measures 122 mm × 79 mm × 29.5 mm, offers a spectral resolution of 1 nm, and can be connected and controlled via the USB port of a computer. Once the setup process reaches its final stage, the computer establishes a connection with the spectrometer. The advanced software application from Thorlabs displays both Before storing this data, SPR curves and the associated data values are displayed in real time on the computer screen. **Fig. 7** illustrates the optical fiber chemical sensor based on SPR experimental configuration that includes a carbon quantum dots coating.

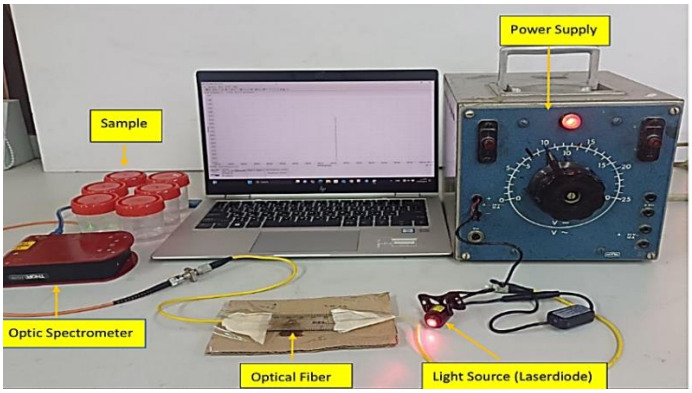

Figure 7. Experimental setup of the optical fiber chemical sensor's SPR

4.7 Preparation of Solutions of Different Refractive Indices

The sensor detects a range of refractive indices (n_s) when exposed to sucrose/water mixtures of various concentrations. The refractive indices for these mixtures were determined using an Abbe refractometer. **Fig. 8** shows that the refractive index

demonstrates a linear relationship with solution concentration. these results align with **(Abbas and Ahmed, 2024).** Sucrose/water mixtures were used to calibrate the sensor, while acetic acid solutions were tested to evaluate the sensor's chemical sensing ability.

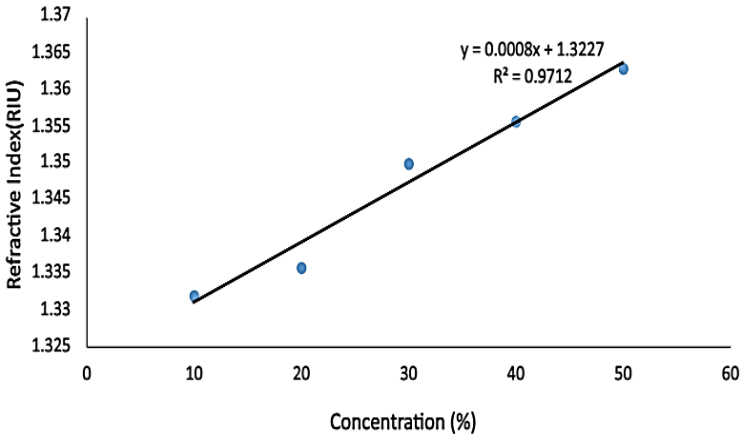

Figure 8. The RI vs. % of sucrose concentrations, with results obtained using a refractometer.

5. RESULTS AND DISCUSSION

A single-mode optical fiber (SMF) was employed, in which the cladding was chemically etched using hydrofluoric acid (HF) to expose the core. This procedure was applied in both numerical simulations and experimental investigations. The exposed section received a 13.1 μm-thick carbon quantum dot coating to improve the fiber's chemical sensitivity. Sucrose/water mixture samples showed a refractive index range between 1.334 and 1.363. Researchers measured light transmission through the optical cable to gather spectral data. **Fig. 9** shows that the T-wavelength corresponds with the surface plasmon resonance (SPR) curve where each specific wavelength reveals the resonance wavelength. Material transmission (T) results from dividing the measured light intensity of a sample by the optical signal intensity in the air **(Jassam et al., 2024)**. Transmission (T) is influenced by wavelength (nm). **Fig. 10** shows that the Spectrum of the polychromatic light through the sensor measured different acetic acid using the spectrum analyzer. The sensor with carbon-quantum dot layers demonstrated surface plasmon resonance (SPR) across different chemical sample refractive indices, as shown in **Fig. 11**.

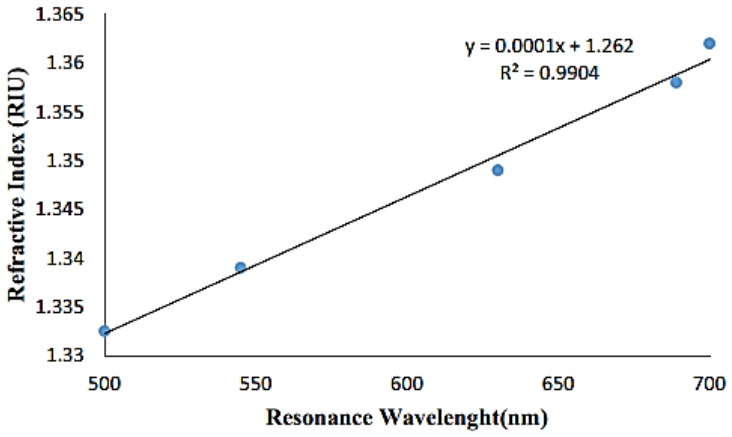

Figure 9. The carbon-layered sensor's refractive index in connection with the resonance wavelength.

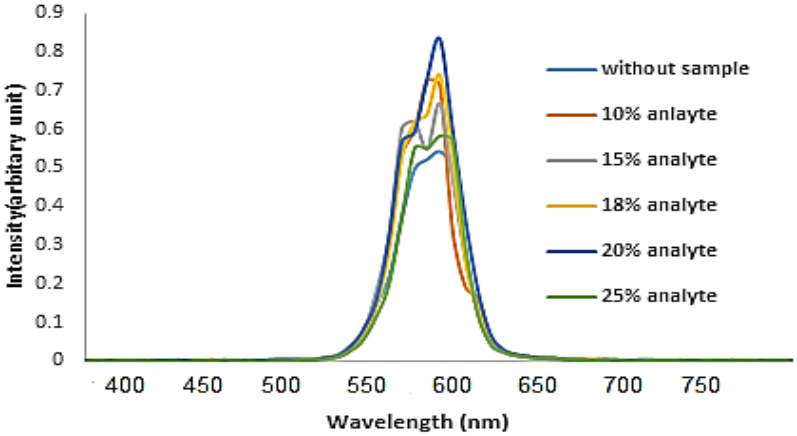

Figure 10. Spectrum of the polychromatic light through the sensor measured different acetic acid using the spectrum analyzer

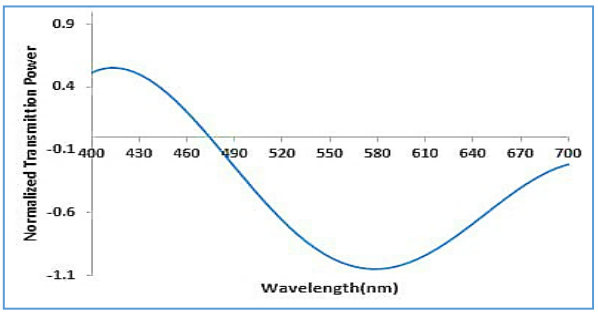

a- acetic acid (10%)

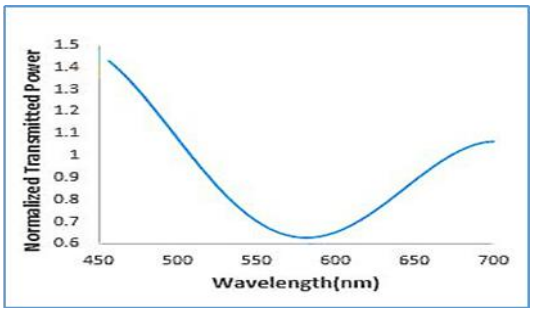

b- acetic acid (15%)

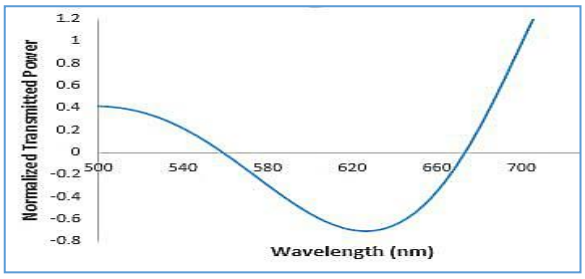

c- acetic acid (18%)

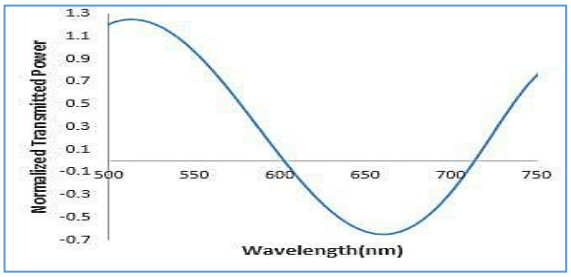

d- acetic acid (20%)

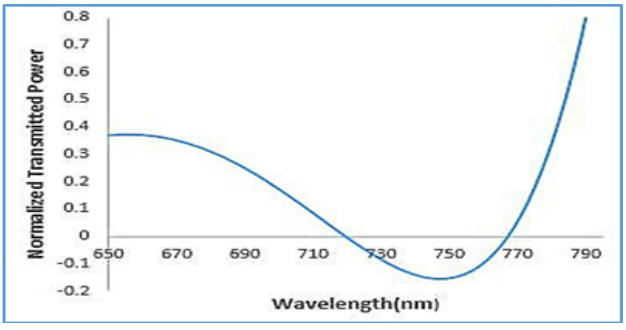

e- acetic acid (25%)

Figure 11. SPR curve of the carbon quantum dot-equipped chemical optical fiber sensor for varying acetic acid concentrations.

The SPR response curves show differences in both width and dip position based on which sensor is used because the refractive index varies between samples. The magnitude of dip position movement expands as the refractive index rises. The performance metrics vary under changes in the resonance wavelength and refractive index of the sensing medium since these metrics depend on the shifting value, dip location and the SPR curve's width. Performance parameters change when the spectral curve width and resonance wavelength, along with the refractive index, undergo alterations. As the refractive index increases, the SPR dip shifts to longer wavelengths while becoming shallower and broader due to increased damping and changes in electron distribution in the CQD layer.

Experimental results of the constructed sensors with carbon layers and simulated sensors with carbon layers are illustrated within **Table 1**. **Table 2** shows each acetic acid sample's refractive index and concentration information at various resonance frequencies. presented. The study in **(Zhou et al., 2025)** demonstrates that higher sample concentration, along with greater refractive index, results in resonance wavelength shifts. The transition is marked by an abrupt extension toward longer red wavelengths. In this work, the sensor's sensitivity was mainly calculated based on the resonance wavelength shifts, due to their consistency and reliability across measurements. The negative transmission values observed in **Fig. 11 (a–e)** are due to comparison with the reference spectrum and indicate reduced intensity, not true negative transmission. Small differences in the measurement conditions are responsible for the small deviation observed in **Fig. 11(b).**

Table 1. The carbon sensor's measurements of experimental performance.

Nanomaterial	(Sn)Sensitivity [μm/RIU]	Signal-to-noise ratio (SNR)	Merit figure (FOM)	[RIU] Resolution
Carbon	10	0.14	140	$1*10^{-4}$

Table 2. Resonance frequencies for various concentration levels and refractive indices of acetic acid were measured.

Concentration (C) (%)	10%	15%	18%	20%	25%
Resonance Wavelength (λ_{res})(nm)	580	590	620	650	750
Refractive Index (n) (RIU)	1.32	1.321	1.324	1.327	1.337

6. CONCLUSIONS

The carbon-coated optical sensor demonstrated good sensitivity in detecting changes in the concentration of acetic acid. The resonance wavelength was shifted by variations in the surrounding mediums refractive index, and it gradually red-shifted as concentration increased. Spectral and intensity analyses were employed to assess the sensor's performance, which revealed a signal-to-noise ratio of 0.14 and a sensitivity of 10 μm/RIU.

Credit Authorship Contribution Statement

Ola Mahdi Alwan helped write the text and prepared the chemical sensors. Soudad S. Ahmed oversaw the research, analyzed the data, and revised the manuscript.

Declaration of Competing Interest

The authors declare that they have no known competing financial interests or personal relationships that could have appeared to influence the work reported in this paper.

REFERENCES

Abbas, F.F., and Ahmed, S.S., 2023. Photonic crystal fiber pollution sensor based on surface plasmon resonance. *Iraqi Journal of Science*, 64(2), pp. 658–667. https://doi.org/10.24996/ijs.2023.64.2.15

Abbas, S.K., and Ahmed, S.A., 2024. Refractive index sensor based on tapered photonic crystal fiber to determine the performance of different carbonated liquids. *Journal of Optics,* 53(3), pp. 2726-2730. https://doi.org/10.1007/s12596-023-01489-z

Abd, A.H., and Ibrahim, O.A., 2022. Synthesis of carbon quantum dot by electro-chemical method and studying optical, electrical, and structural properties. *Chemical Methodologies*, 6(11), pp. 823–830. https://doi.org/10.22034/CHEMM.2022.351559.1575

Abdul Kareem, M.J., and Ahmed, S.S., 2023. Surface plasmon resonance (SPR)-based multimode optical fiber sensors for electrical transformer oil aging detection. *Iraqi Journal of Physics,* 21(4), pp. 84–91.

Ateia, E. E., Rabie, O., and Mohamed, A. T. ,2024. Assessment of the correlation between optical properties and CQD preparation approaches. *The European Physical Journal Plus*, 139(1), pp. 1-12 https://doi.org/10.1140/epjp/s13360-023-04811-7

Baker, S.N., and Baker, G.A., 2010. Luminescent carbon nanodots: emergent nanolights. *Angewandte Chemie International Edition*, 49(38), pp. 6726–6744. https://doi.org/10.1002/anie.200906623

Daniyal, W.M.E.M.M., Yap, W.F., Kariming, M.Z., Muhamad Fauzi, N.I., Hashim, H.S., Anuar, M.F., Nugroho, F.A.A., Hidayat, N., Abdullah, H., Taufiq, A., and Kamal Eddin, F.B., 2025. Enhanced surface plasmon resonance detection of ascorbic acid using carbon quantum dots thin film. *Plasmonics,* pp. 1-12. https://doi.org/10.1007/s11468-025-03194-y

Ding, J., Yang, L., Chen, Q., Zhang, L., and Zhou, P.,2017. Demonstration of a directed XNOR/XOR optical logic circuit based on silicon Mach–Zehnder interferometer. *Optics Communications,* 395, pp. 183-187. https://doi.org/10.1016/j.optcom.2015.08.024

Gupta, B.D., 2006. Fiber Optic Sensors: Principles and Applications. *New Delhi, India: New India Publishing.*

He, S., Li, M., Liu, Y., and Pan, Y., 2008. Carbon nanotube-coated optical fiber sensors. *Sensors and Actuators B: Chemical*, 133(2), pp. 370–373. https://doi.org/10.1016/j.snb.2008.03.004Y.

Homola, J.,1995. Optical fiber sensor based on surface plasmon excitation. *Sensors and Actuators B: Chemical,* 29(1–3), pp. 401–405, https://doi.org/10.1016/0925 4005(95)01714 3

Hottin, J., Wijaya, E., Hay, L., Maricot, S., Bouazaoui, M., and Vilcot, J.-P., 2013. Comparison of gold and silver/gold bimetallic surface for highly sensitive near-infrared SPR sensor at 1550 nm. *Plasmonics*, 8(2), pp. 619–624. https://doi.org/10.1007/S11468-012-9446-1

Jassam, G. M. ,2024. Refractive index sensor based on tapered optical fiber to determine the performance of different copper samples. *Journal of Optics*, pp. 1-5. https://doi.org/10.1007/s12596-024-02373-0

Jassam, G. M., Abbas, Z. A., and Mohammed, S. H., 2024. Single mode optical fiber sensor based on surface plasmon resonance for the detection of the Lactic acid for the chemical sensor. *Journal of Optics*, pp. 1-4. https://doi.org/10.1007/s12596-024-02211-3

Jassam, G.M., Abdaldeen, Z. K., Taboor, R. M., and Benchaabane, A., 2024. Plastic optical fiber sensor for sensing refractive index of citric acid based on surface plasmon resonance. *Al-Nahrain Journal of Science*, 27(2), pp. 114–118. https://anjs.edu.iq/index.php/anjs/article/view/2749

Jiang, J., Zhang, C., Li, Z., 2021. Snapshots into carbon dots formation through a combined structural, chemical and photophysical investigation. *Nature Communications*, 12, pp. 1–11.

Jorgenson, R. C., and Yee, S. S., 1993. A fiber-optic chemical sensor based on surface plasmon resonance*, Sensors and Actuators B: Chemical,* 12(3), pp. 213–220. https://doi.org/10.1016/0925-4005(93)80021-3

Jorgenson, R. C., and Yee, S. S., 1993. Multi-wavelength surface plasmon resonance as an optical sensor for characterizing the complex refractive indices of chemical samples. *Sensors and Actuators B: Chemical,* 14(1–3), pp. 721–722. https://doi.org/10.1016/0925-4005(95)85158-5

Kumawat, M.K., Thakur, M., Gurung, R.B., and Srivastava, R., 2019. Graphene quantum dots for cell proliferation, nucleus imaging, and photoluminescent sensing applications. *Scientific Reports*, 9(1), P. 5008.

Li, X., Rui, M., Song, J., Shen, Z., and Zeng, H., 2020. Carbon and graphene quantum dots for optoelectronic and energy devices. A review. *Advanced Functional Materials*, 25(31), pp. 4929–4947. https://doi.org/10.1002/adfm.201501250

Low, T., and Avouris, P., 2014. Graphene plasmonics for terahertz to mid-infrared applications. *ACS Nano,* 8(2), pp. 1086–1101. https://pubs.acs.org/doi/abs/10.1021/nn406627u.

Mahmood, A. I., and Ahmed, S. S., 2018. Refractive index sensor based on micro-structured optical fibers with using finite element method. *Iraqi Journal of Science*, 59(3C), pp. 1577–1586.

Nesterenko, D.V., and Sekkat, Z., 2013. Resolution estimation of the Au, Ag, Cu, and Al single- and double-layer surface plasmon sensors in the ultraviolet, visible, and infrared regions*. Plasmonics,* 8(4), pp. 1585–1595. https://doi.org/10.1007/s11468-013-9575-17

Nacpil, E. J. C., Wang, Z., Zheng, R., Kaizuka, T., and Nakano, K.., 2019. Design and evaluation of a surface electromyography-controlled steering assistance interface. *Sensors*, 19(6), P. 1308. https://doi.org/10.3390/s19061308

Rigodanza, F., Burian, M., Arcudi, F., Đorđević, L., Amenitsch, H., and Prato, M., 2021. Snapshots into carbon dots formation through a combined structural, chemical and photophysical investigation. *Nature Communications*, 12, pp. 1–11. https://doi.org/10.1038/s41467-021-22902-w

Srivastava, K., and Gupta, B.D., 2011. Influence of ions on the surface plasmon resonance spectrum of a fiber optic refractive index sensor. *Sensors and Actuators B: Chemical*, 156(2), pp. 559–562. https://doi.org/10.1016/j.snb.2011.04.070.

Thakur, A., and Kumar, A., 2024. Challenges and opportunities in the development of nano-hybrid smart coatings. *Nano-Hybrid Smart Coatings: Advancements in Industrial Efficiency and Corrosion Resistance*, pp. 353-384. https://doi.org/10.1021/bk-2024-1469.ch015

Tuerhong, M., Xu, Y., and Li, X., 2022. Carbon dots: classification, properties, synthesis, characterization and applications (Review). *RSC Advances*, 12, pp. 11185–11207.

Urrutia, A., Goicoechea, J., and Arregui, F.J., 2015. Optical fiber sensors based on nanoparticle-embedded coatings. *Journal of Sensors*, (Article ID 805053), pp. 1-18. https://doi.org/10.1155/2015/805053.

Wang, Y., and Hu, A., 2019. Carbon quantum dots: synthesis, properties and applications. *Journal of Materials Chemistry C*, 7(31), pp. 7176–7191. https://doi.org/10.1039/C4TC00988F

Wang, Y., Kalytchuk, S., Zhang, Y., Shi, H., Kershaw, S.V., and Rogach, A.L., 2021. Carbon dots in sensing and bioimaging: a review. *Journal of Materials Chemistry* C, 9(2), pp. 491–507.

Wu, D., Wu, Y., Xu, Y., Liu, Y., Wang, P., and Yang, G., 2016. Carbon quantum dots in optical fiber sensing. *Analytical Chemistry*, 88(23), pp. 11700–11706.

Xu, Y., Wu, Y., Liu, Y., Wang, P., Fang, Y., and Xiao, S., 2014. Carbon quantum dots: synthesis, properties and applications. *Journal of Materials Chemistry C*, 2(34), pp. 6694–6703. https://doi.org/10.1039/C4TC00988F.

Yan, H., Low, T., Zhu, W., Wu, Y., Freitag, M., Li, X., and Avouris, P., 2013. Damping pathways of mid-infrared plasmons in graphene nanostructures. *Nature Photonics*, 7(5), pp. 394–399. https://doi.org/10.1038/nphoton.2013.57.

Yao, Y., Liu, Y., Wang, P., Fang, Y., and Xiao, S., 2020. Surface functionalization of optical fibers with carbon materials. *Journal of Lightwave Technology*, 38(12), pp. 3103–3110.

Yasser, N., Ali, N. A., and Sulaiman, L. H. ,2018. Polymer optical fiber sensor side-pumped with polymer clad doped lasing compounds. *Iraqi Journal of Science*, 59(1B), pp. 294–298. https://doi.org/10.24996/ijs.2018.59.1B.15

Yola, M.L., and Atar, N., 2020. A novel electrochemical sensor based on carbon quantum dots and graphene oxide hybrid for sensitive detection of biomolecules. *ACS Sensors*, 5(7), pp. 1832–1839.

Zhou, Y., Camisasca, A., Dominguez-Gil, S., Bartkowski, M., and Giordani, S., 2025. Synthesis of carbon quantum dots from spent coffee grounds. *transforming waste into potential biomedical tools. Nanoscale*. https://doi.org/10.1039/d4nr05186f

Zhu, S., Meng, Q., Wang, L., Zhang, J., Song, Y., Jin, H., … and Yang, B., 2015. Highly photoluminescent carbon dots for multicolor patterning, sensors, and bioimaging. *Angewandte Chemie International Edition*, 52(14), pp. 3953–3957. https://doi.org/10.1002/anie.201300519

الألياف الضوئية أحادية الوضع مطلية بنقط الكربون الكمومية لتطبيقات الاستشعار الكيميائي

علا مهدي علوان*، سؤدد سلمان أحمد

قسم الفيزياء، كلية العلوم، جامعة بغداد، بغداد، العراق

الخلاصة

يصف هذا العمل تطوير مستشعر ألياف ضوئية أحادي الوضع يمكنه اكتشاف تركيزات مختلفة من محاليل حمض الأسيتيك. تم استخدام حمض الهيدروفلوريك (HF) لحفر كسوة الألياف كيميائيا لفضح قلبها، الذي تلقى طبقة من النقاط الكمومية الكربونية. خضع المستشعر للاختبار بخمسة تركيزات من حمض الأسيتيك بنسبة 10٪ و15٪ و18٪ و20٪ و25٪ لتحديد حساسيته من خلال اختلافات الطول الموجي بالرنين وتغيرات نقل الضوء. أظهر المستشعر تحولا أحمر واضحا في الطول الموجي للرنين عند تعرضه لتركيزات أعلى، مما أظهر علاقة واضحة بين معامل الانكسار لوسط الاستشعار والاستجابة البصرية للمستشعر. هناك حاجة متزايدة لطريقة مدمجة وعالية الحساسية لاكتشاف حمض الخليك، حيث إن التقنيات التقليدية غالبًا ما تعاني من حساسية منخفضة وأجهزة كبيرة الحجم. أكدت التحليلات الطيفية والشدة أداء المستشعر، حيث أظهرت قياس حساسية قدره 10 ميكرومتر / RIU ونسبة ثابتة من الإشارة إلى الضوضاء تبلغ 0.14. تعتمد آلية الاستشعار بشكل أساسي على رنين البلازمون السطحي (SPR)، الذي يتم تمكينه من خلال التفاعل بين المجال الزائل للألياف وطلاء النقطة الكمومية الكربونية. تثبت نتائج الاختبار أن المستشعر يعمل بكفاءة في الكشف عن المواد الكيميائية السائلة، وخاصة حمض الأسيتيك والمواد العضوية ذات الصلة، باستخدام معدات مخروطة مصممة خصيصًا، مما يزيد بشكل كبير من حساسيته لمعامل الانكسار المحيط. في مركز الحساس، تم إنشاء جزء صغير (4 سم) من الألياف أحادية الوضع (SMF) بمقاسات مخروطة معدلة، وتم غمر غلاف الألياف في تركيزات مختلفة من عينة حمض الخليك لاستشعار تغيّرات معامل الانكسار الفعال (RI).

الكلمات المفتاحية: الالياف أحادية الوضع، رنين البلازمون السطحي، استشعار حمض الاسيتيك.